Iranian Journal of Medical Physics
Vol. 14, No. 1, March 2017, 15-22
Received: September 27, 2016; Accepted: January 09, 2017

Original Article

Numerical Study for Optimizing Parameters of High-Intensity Focused Ultrasound-Induced Thermal Field during Liver Tumor Ablation: HIFU Simulator

Somayeh Gharloghi[1], Mehrdad Gholami[2], Abbas Haghparast[1], Vahab Dehlaghi[1*]

Abstract

Introduction
High intensity focused ultrasound (HIFU) is considered a noninvasive and effective technique for tumor ablation. Frequency and acoustic power are the most effective parameters for temperature distribution and the extent of tissue damage. The aim of this study was to optimize the operating transducer parameters such as frequency and input power in order to acquire suitable temperature and thermal dose distribution in the course of a numerical assessment.

Materials and Methods
To model the sound propagation, the Khokhlov-Zabolotskava-Kuznetsov (KZK) nonlinear wave equation was used and simulation was carried out using MATLAB HIFU toolbox. Bioheat equation was applied to calculate the transient temperature in the liver tissue. Frequency ranges of 2, 3, 4, and 5 MHz and power levels of 50 and 100 W were applied using an extracorporeal transducer.

Results
Using a frequency of 2 MHz, the maximum temperatures reached 53°C and 90°C in the focal point for power levels of 50 W and 100 W, respectively. With the same powers and using a frequency of 3 MHz, the temperature reached to 71°C and 170°C, respectively. In addition, for these power levels at the frequency of 4 MHz, the temperature reached to 72°C and 145°C, respectively. However, at the 5 MHz frequency, the temperature in the focal spot was either 57°C or 79°C.

Conclusion
Use of frequency of 2 MHz and power of 100 W led to higher thermal dose distribution, and subsequently, reduction of the treatment duration and complications at the same exposure time in ablation of large tumors.

Keywords: High-Intensity Focused Ultrasound Ablation, Nonlinearity KZK Equation, Optimization, Thermal Dose

1- Department ofMedical Physics & Biomedical Engineering, School of Medicine, Kermanshah University of Medical Sciences, Kermanshah, Iran
2- Department of Medical Physics, Lorestan University of Medical Sciences, Khorramabad, Iran

*Corresponding author: Tel: 09188305608; Email: Dr.dehlaqi@yahoo.com

1. Introduction

Liver and intra-hepatic bile duct cancers are considered as major human health problems and the second most frequent causes of mortality in Asia [1]. Reports showed that 30% of patients suffer from metastatic disorders in the liver during diagnosis. It is also shown that about 50% of cancers extend at the time of Sickness
. Thus, the first-line treatment for this condition is mostly hepatic resection or liver transplantation that unfortunately only 10-25% of patients can undergo the curative resection. It is estimated that five-year survival is possible only for 4 0% of the patients [2].

Currently, minimally invasive and noninvasive thermal therapy techniques consisting of laser, radiofrequency ablation (RFA), microwave, and high intensity focused ultrasound (HIFU) are used as a substitute for surgery and radiotherapy [3].

Unlike other minimally invasive procedures, HIFU is an extracorporeal and entirely noninvasive modality for tumor ablation with a typically short patient recovery time. The primary advantages of HIFU beam are high ability to converge and deliver thermal energy into the localized target volume with sub-millimeter accuracy and non-ionizing nature, which makes treatment safe [4, 5]. The fast conversion of acoustic energy to heat can elevate tissue temperature of a specific area and lead to irreversible damages and cell death [6].

In comparison with several-minute duration in other modalities, HIFU procedure releases a considerable amount of thermal energy into a finite volume and causes an instantaneous temperature rise during only a few seconds [7]. Maximum temperature is induced at the focal point, and other points are also exposed to various heat levels depending on physiological characteristics and its relative place from the face of the transducer [7, 8].

The cancerous tissue temperature is elevated to higher than 60°C within a few seconds and can lead to irreversible cell death via coagulation necrosis [9]. In principle, when the tissue temperature exceeds 55°C, cell necrosis and lethal bioeffects occur. Temperatures above 95°C can lead to cavitation and boiling with high extents of lesion (coagulated necrosis zone) that cannot be evaluated correctly [3]. Heat control in targeted volume depends on power levels, acoustical intensity, and frequency that affect temperature distribution [10].

In previous studies, HIFU was simulated in various amplitudes and by continuous and pulsed waves at 1 MHz frequency. However, they did not take into account the effects of nonlinearity to estimate necrotic volumes. In addition, since the heat levels were estimated just from the thermal aspect, the lesion size and shape were not accurately predicted [3, 6].

Therefore, by considering the nonlinearity effects of HIFU waves, the aim of this study was to optimize the operational transducer parameters such as frequency and power to acquire suitable temperature and thermal dose distributions in a simulation assessment.

2. Materials and Methods

Simulation of ultrasound propagation plays an important role in the advancement of HIFU technology [11]. One interesting method to simulate nonlinear propagation was the Khokhlov-Zabolotskava-Kuznetsov (KZK) nonlinear parabolic wave equation describing axisymmetric acoustic propagation [12]. The KZK parabolic equation is the simpler derivation of Westervelt model that has a different time frame [13]. This equation takes into account absorption, diffraction, and nonlinearity effects of sound propagation in thermo-viscous tissues [14]:

$$\frac{\partial^2 P}{\partial z \partial \tau} - \frac{c_0}{2}\nabla_{\perp}^2 P - \frac{\delta}{2c_0^3}\frac{\partial^3 P}{\partial \tau^3} - \frac{\beta}{\rho c_0^3}\frac{\partial^2 P^2}{\partial \tau^2} \qquad (1)$$

Where P is the acoustic pressure, ρ is the density, $\beta = 1 + \frac{B}{2A}$ is the coefficient of nonlinearity with $\frac{B}{A}$ being the nonlinear parameter 6.6 and 3.5 for liver and water, respectively. c_0 is the small signal sound speed, $\tau = t - \frac{z}{c_0}$ is the new time frame, and z is the coordinate of direction of propagation also the diffusivity of sound, δ accounts thermal and

viscous losses in thermo-viscous soft tissues and is defined below [3, 15, 16].

$$\delta = \frac{2c_0^3\alpha}{\omega^2} \quad (2)$$

where α and ω indicate the acoustic absorption coefficient and angular frequency of the signal, respectively.

Ultrasound intensity can be exponentially attenuated when passing through the biological tissue. Attenuation coefficient follows the power-law frequency dependence of the form $\alpha(f)= \alpha_0.f^{\eta}$. Where α_0 is absorption coefficient (at reference frequency of 1 MHz), and f and η are frequency and material specific parameters typically in the range $1\leq\eta\leq2$, respectively. In this consensus η for the liver and water was equal to 1.1 and 2, respectively [15, 17, 18]. Therefore, the attenuation coefficient and nonlinear properties are different for various tissues.

All simulations were implemented in MATLAB R2013a (the Mathworks, Inc., Natick, MA) powerful software environment, using HIFU simulator toolbox approved by Food and Drug Administration (FDA). Acoustic pressure field was solved using second-order diagonally implicit Runge-Kutta and Crank-Nicolson finite-difference operators for integrating the kth (k=128) harmonic equation. In this study, the time domain was used based on implementation of KZK [19].

Volumetric heat rate (Q_s [W/m^3]) was directly obtained from pressure field distribution pointed out below and was assumed to be proportional to acoustic intensity I [20].

$$Q_s = 2\alpha I \quad (3)$$

Intensity (I [W/m^2]) in the prior equation can be written in terms of P:

$$I = \frac{P^2}{2\rho C_0} \quad (4)$$

A single element with a 2.5 cm aperture, 2 cm diameter hole in the center of transducer, and focal length of 10 cm was applied.

The applied frequencies of 2, 3, 4, and 5 MHz with 50 and 100 W emitted acoustic powers were also employed. To reduce the reflective effects of the sound, transducer was modeled in water. In our model, after travelling 5 cm in water the waves reached to the interface of perfused liver tissue. The sound reflection was 0.2% that was a very insignificant value. The simulated exposure sequence consists of 5 pulses including an initial 0.3 s pulse duration followed by four pulses of 0.1 s at 0.5 s interval time. Heating phase was then followed by about 5 s of cooling phase. Additionally, duty factor of exposure was 20%. Definition of the duty factor is [21]:

$$\text{Duty factor} = \frac{\text{Pulse Duration}}{\text{Pulse Repetition Rate}} \quad (5)$$

Temperature elevation most commonly can be determined by the Pennes bioheat transfer equation [20]:

$$\rho c \frac{\partial T}{\partial t} = \nabla\, k.\nabla T - w_{bl}c_{bl}(T - T_{bl}) + Q_s \quad (6)$$

Where ρ is density, c is the specific heat capacity, k denotes constant thermal conductivity, W_{bl} is the blood mass perfusion rate (W_{bl}=15 Kg/m^3.s), C_{bl} is specific heat capacity of the blood, T_{bl} is temperature of inflowing arterial blood, that is assumed equal to 37°C, and Q_s is power deposition per unit volume as defined previously [5].

Bioheat equation is one of the prevalent methods for calculating the temperature rise during exposure. This equation takes into account influence of the blood flow in the capillary bed. Several studies were performed to investigate the effects of large blood vessels on temperature distribution [3, 6]. Solovchuk et al. considered the effect of blood flow cooling and acoustic streaming on the temperature rise and coagulated necrosis volume [3].

A finite-difference time domain (FDTD) method was employed to compute the sound and heat equations for both water and liver domains [12, 13]. Physical properties of the biological tissues used in the simulations are listed in Table 1 [5, 15, 16, 19, 22-24].

HIFU-induced temperature fields were applied to compute the thermal dose (TD) and lesion volumes. This procedure was developed by Sapareto and Dewey [25]. It was indicated that an exponential relationship exists between tissue temperature and required exposure time for annihilating the cells and formation of coagulated necrosis volumes. The thermal dose is obtained as:

$$TD_{43(x,y,z)} = \int_0^t R^{43^{\circ}C-T(t)} dt \qquad (7)$$

where R= 0.5 for T≥43°C and R=0.25 for T<43°C.

According to this equation, thermal dose resulting from heating the tissue to 43°C for 240 min is equivalent to what is achieved by heating to 56°C for 1.76 s [6]. Thermal dose of $100<t_{43}<1000$ min at 43°C can bring about irreversible damages and induce coagulated necrosis [5].

Table 1. Acoustic and thermal properties for biological tissues

Material properties	Units	Symbol	Liver	Water
Density	kg/m^3	ρ	1060	1000
Sound speed	m/s	c_0	1595	1482
Thermal conductivity	W/m.K	k	0.51	0.6
Specific heat capacity	J/kg.K	c	3639	4180
Attenuation coefficient of sound	dB/m	α_0	50	0.217

3. Results

To compute the induced heat to the liver tissue, measurements were carried out using different frequencies and power levels. Nonlinear behavior was investigated for 128 wave harmonics; there are both positive and negative pressure peaks in pressure curves. The pressure peaks cover those points. Moreover, there are some short pressure peaks before the large amplitude peak, which cause partial thermal field. Comparison between the pressure amplitude distributions is shown in Figure 1.

Furthermore, due to the relative phase shift between harmonic components of distorted wave caused by diffraction, the positive and negative peak pressures were asymmetric [26]. In the similar power level, amplitude of the produced pressure peaks at 3 MHz frequency was greater than other frequencies at the focal depth of 10 cm of the liver.

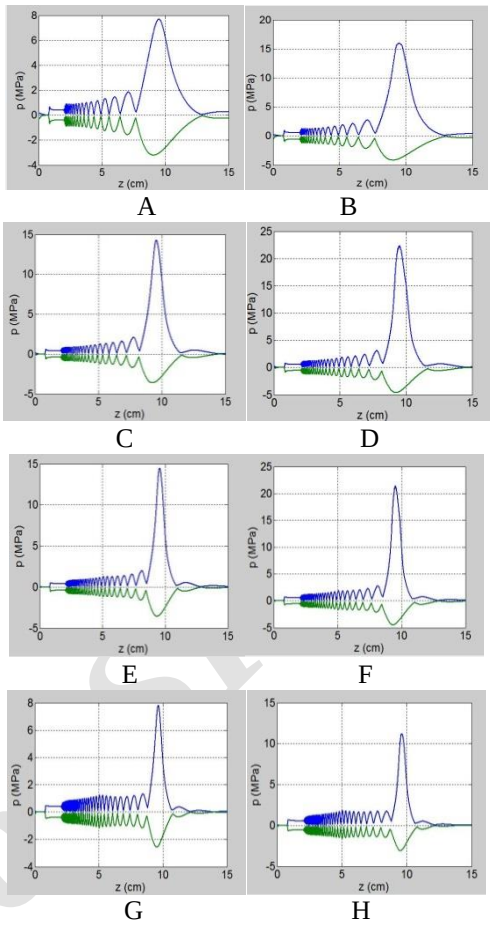

Figure 1. Axial peak positive and negative pressures at different frequencies and emitted acoustic powers of (A) 2 MHz, 50 W; (B) 2 MHz, 100 W; (C) 3 MHz, 50 W; (D) 3MHz, 100 W; (E) 4 MHz, 50 W; (F) 4 MHz, 100 W; (G) 5 MHz, 50 W; (H) 5 MHz, 100 W

As shown in all the figures, there is a sound displacement from the geometrical focus toward the transducer face due to diffraction effect. In some studies, it was demonstrated that Q_s is proportional to P^2 [20], and the Q_s curves were approximately similar to pressure curves.

As shown in Figure 2, the temperature increased at the focal spot. At 2 MHz frequency, the maximum temperature in the focal point reached 53°C and 90°C for both 50 W and 100 W powers, respectively. At 3 MHz frequency and similar powers, temperature reached to 71°C and 170°C. Furthermore, the temperature reached to 72°C and 145°C at 4 MHz frequency. However, at 5 MHz frequency the temperature reached to 57°C and 79°C.

In addition, it can be noted that the temperature peak was the highest at t=0.38 s. Because of the

first pulse duration (0.3 s), the temperature elevation of the first pulse had the highest value in total curves. We compared these profiles with each other and selected with temperature peaks of 60-95°C.

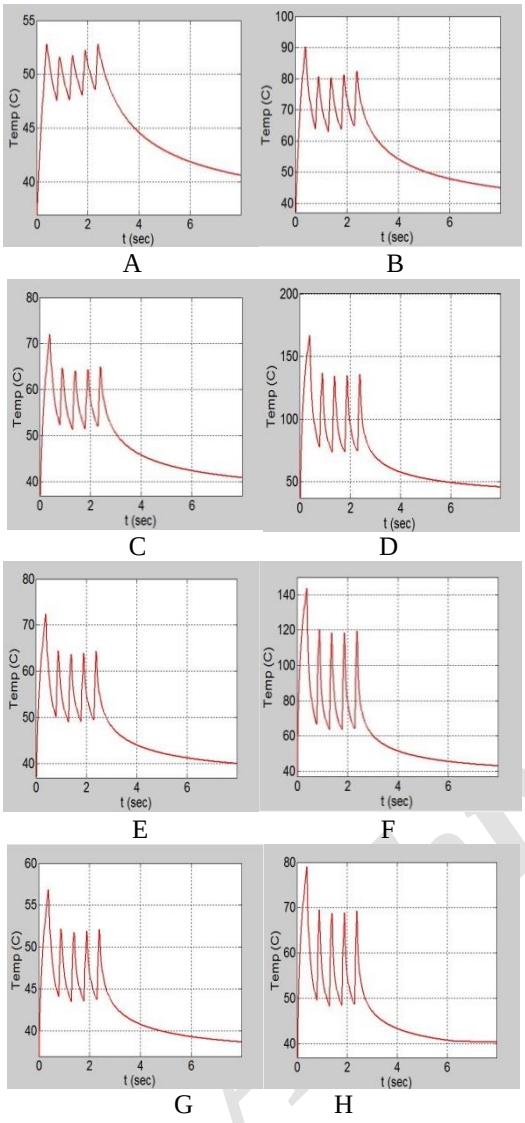

Figure 2. Simulated peak temperature as a function of time at frequencies and emitted acoustic powers of (a) 2 MHz, 50 W; (b) 2 MHz, 100 W; (c) 3 MHz, 50 W; (d) 3 MHz, 100 W; (e) 4 MHz, 50 W; (f) 4 MHz, 100 W; (g) 5 MHz, 50 W; (h) 5 MHz, 100 W

At 3 and 4 MHz frequencies with 100 W powers, increasing the temperature above 95°C can cause both thermal and mechanical effects. However, because the mechanical effects were not considered in calculations, we did not obtain these results.

In Figure 3, predictions of intensity profiles and spatial temperature distribution are shown for four cases composed of previously mentioned condition along the ultrasound propagation and radial axis.

The remaining cases were excluded from our assessment. There was a steep gradient of temperature along the width of the beam in comparison with the temperature gradient across the length.

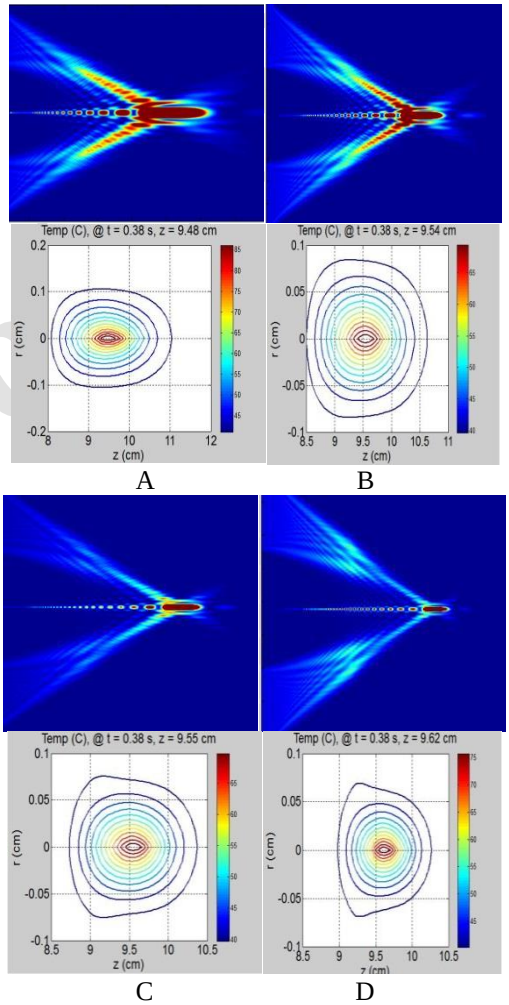

Figure 3. Predicted intensity profiles and temperature contours at frequencies and emitted acoustic powers of (A) 2 MHz, 100 W; (B) 3 MHz, 50 W; (C) 4 MHz, 50 W (D) 5 MHz, 100 W

The thermal dose profiles were calculated by using the above-mentioned temperature contours and are showed in Figure 4. The thermal build-up accumulation is observed at the end of the

first sonication. In this study, predicted lesion volumes with temperatures above 95°C were not shown. Consequently, they are computed without considering the mechanical effect. Thus, because of limitation in our computation, there is no certainty in lesion volume yields from 3 and 4 MHz frequencies and 100 W power transducers. In addition, the physical parameters of transducer can affect size and shape of the necrosis volume induced by HIFU therapy.

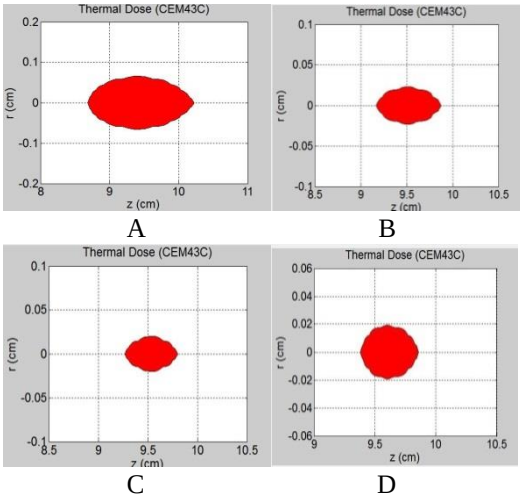

Figure 4. Radial and axial depths of ablation zone as indicated by thermal dose TD_{43}

4. Discussion

The real therapy condition and focal energy delivery can be established by the nonlinear effect. The effect of nonlinearity on the acoustic pressure calculation and temperature response has been previously investigated [12]. Acoustical frequency is generally considered as the most important parameter in therapeutic ultrasound applications [7]. It is well known that the ultrasound attenuation increases with frequency; accordingly, high frequencies could not be used for the treatment of deep-seated tumors. The acoustic power was also another effective parameter. In general, high power levels have more ability to induce the high temperatures within a few seconds [27].

The pressure peak values were between the 8 and 22.5 MPa, while the maximum pressure peak was at 3 MHz frequency and 100 W power in the focal depth. It should be mentioned that frequency and power changes had significant effects on the pressure distribution inside the liver tissue. Increased frequency causes the focal region and acoustic pressure curves become smaller and narrower, respectively. It is evident that pressure peak increases with power. As shown in Figure 1, frequency enhancement from 2 to 4 MHz results in an increase in the pressure peak value at power of 100 W, although it was decreased at frequency of 5 MHz. These results were not observed using the power of 50 W.

It was indicated that increased ultrasound intensity elevates the temperature peak; thus, the lowest focal temperature peak was close to 53°C at the first pulse at 2 MHz frequency and 50 W power (Figure 2-a). Then, by comparing the related temperature contours and their thermal doses, their optimal distributions were achieved. In fact, the HIFU-induced thermal doses and discrepancies between their lesion volumes were clearly distinguishable.

Regardless of cavitation phenomenon, the lesion size and shape can be well-predicted exclusively from the thermal and nonlinearity aspects. Recently, Solovchuk et al. showed that lesion size was obtained by solely taking into account the thermal effects. The maximum temperature never exceeded 95°C, which indicated absence of any mechanical effects of ultrasound waves such as cavitation [3]. Lesion size can be increased with inertial cavitation that significantly enhanced heat deposition at the HIFU focus [20]. In our study, we investigated the effect of higher powers (50 and 100 W) and frequencies higher than 1 MHz on thermal distribution. Furthermore, we measured the lesion volume at various frequencies.

Because each 3 s of sonication includes four short pulses and produces higher transient temperatures, thermal volume dose is considerable. In similar studies, for producing these situations, more sonications are applyied. The reported thermal doses were compared to obtain the suitable exposure condition. The minimum and maximum widths of necrotic

zones at z direction were obtained at 2 and 5 MHz frequencies (with 100 W power), respectively, which are shown in (Figure 4-D and A). Clearly, a difference between the ablated zone volumes is revealed in the maps. Thus, the minimum and maximum destroyed volumes were obtained at 5 and 2 MHz frequencies (with 100 W power), respectively. The powers and frequencies were tested for reaching the optimal temperature and thermal dose distributions at a pulsed mode sonication. The continuous waves were also utilized in several studies [15, 28]. The large area of coagulated necrosis is rapidly obtained by applying 2 MHz frequency and 100 W power in the same exposure time. In large tumor ablation, it enables us to have a higher destroyed volume at shorter period of time .

Ultrasound therapy has the potential to be combined with imaging devices such as magnetic resonance guided HIFU (MRG HIFU). Moreover, applying MRG HIFU technique can provide effective spatial control and monitoring-induced thermal lesions during HIFU therapies [29-31]. Observed displacement is less at the 5 MHz frequency compared to other frequencies. Thus, higher frequencies can lead to a more accurate sound focus adjacent to geometry focus of the transducer. In conclusion, HIFU parameters were optimized to reduce the treatment time, damage to the surrounding normal structures, and complications in large tumors and to ensure safety and efficacy of this modality.

5. Conclusion

In this numerical assessment, we demonstrated the changes of the transducer parameters such as frequency and power, which show a great impact on the temperature and thermal dose maps. Additionally, we performed a comparative analysis to acquire appropriate geometrical transducer parameters at 2 MHz frequency with 100 W power. In conclusion, utilization of the optimum parameters of transducer can improve the treatment outcome of HIFU to lower the treatment time and present a good protocol for liver therapy.

References

1. Aubry J.F, Pauly B.K, MoonenCh, Haar G.T, Ries M, Salomir R, et al. The road to clinical use of high-intensity focused ultrasound for liver cancer: technical and clinical consensus. Journal of Therapeutic Ultrasound. 2013; 1:13. DOI: 10.1186/2050-5736-1-13.
2. Leslie T, Ritchie R,IllingRT,TerHaar G, Phillips R, Middleton M, et al. High intensity focused ultrasound treatment of liver tumors: post-treatment MRI correlates well with intra-operative estimate of treatment volume. Br JRadiol. 2012; 85 (1018): 1363-70. DOI: 10.1259/bjr/56737365.
3. Solovchuk M.A, Sheu TWH, Thiriet M, Lin WL. On a computational study for investigating acoustic streaming and heating during focused ultrasound ablation of liver tumor. ApplTherm Eng. 2013; 56: 62-76. DOI: 10.1016/j.applthermaleng.2013.02.041.
4. Hudson Th, LooiTh, Waspe A, Drake J, Pichardo S. Simulating temperature distribution of high- intensity focused ultrasound during bone treatments. Journal of Therapeutic Ultrasound. 2015; 3(133). DOI: 10.1186/2050-5736-3-S1-P6.
5. Parkash P, Diederich CJ. Consideration for theoretical modeling of thermal ablation with catheter-based ultrasonic sources: implication for treatment planning, monitoring and control. intJ Hyperthermia. 2012; 28(1): 69-86. DOI: 10.3109/02656736.2011.630337.
6. Banerjee R.K, Dasgupta S. Characterization methods of high intensity focused ultrasound-induced thermal field. Advances Heat Transf. 2012; 42: 137-77. DOI: 10.1016/S0065-2717(10)42002-X.
7. YoshizawaSh, Matsuura K, Takagi R, Yamamoto M, UmemuraSh.I. Detection of tissue coagulation by decorrelation of ultrasonic echo signals in cavitation-enhanced high intensity focused ultrasound treatment. Journal of Therapeutic Ultrasound. 2016; 4:15. DOI: 10.1186/s40349-016-0060-0.
8. Rossi M, Raspanti C, Mazza E, Menchi I, De Gaudio A.R , Naspetti R. High- intensity focused ultrasound provides palliation for liver metastasis causing gastric outlet obstruction: case report. Journal of Therapeutic Ultrasound. 2013; 1:9. DOI: 10.1186/2050-5736-1-9.
9. Zhou Y.F. High intensity focused ultrasound in clinical tumor ablation. World J ClinOncol. 2011; 2(1): 8-27. DOI: 10.5306/wjco.v2.i1.8.

10. Sellani G, Fernandes D, Nahari A, Fabrício de Oliveira M, Valois Ch, Pereira W.C.A, et al. Assessing heating distribution by therapeutic ultrasound on bone phantoms and in vitro human samples using infrared thermotherapy. Journal of Therapeutic Ultrasound. 2016; 4:13. DOI: 10.1186/s40349-016-0058-7.
11. Treeby BE, Jaros J, Rendell AP, Cox BT. Modeling nonlinear ultrasound propagation in heterogeneous media with power law absorption using a k-space pseudo- spectral method. J AcoustSoc Am. 2012; 131(6): 4324-36. DOI: 10.1121/1.4712021.
12. Curra F.P, Mourad P.D, Khokhlova V.A, Cleveland R.O, Crum L.A. Numerical simulation of heating patterns and tissue temperature response due to high-intensity focused ultrasound. IEEE Trans Ultrason, Ferroelectr, Freq Control. 2000; 47(4): 1077-89. DOI: 10.1109/58.852092.
13. Huang J, Holt R.G, Cleveland R.O, Roy R.A. Experimental validation of a tractable numerical model for focused ultrasound heating in flow-through tissue phantoms. J AcoustSoc Am. 2004; 116(4): 2451-8. DOI: 10.1121/1.1787124.
14. Liu X, Li J, Gong X, Zhang D. Nonlinear absorption in biological tissue for high intensity focused ultrasound. Ultrasonics. 2006; 44: 27-30. DOI: 10.1016/j.ultras.2006.06.035.
15. Pulkkinen A, Hynynen K. Computational aspects in high intensity ultrasonic surgery planning. Comput Med Imag Graph. 2010; 34: 69-78. DOI: 10.1016/j.compmedimag.2009.08.001.
16. Duck FA. Propagation of sound through tissue, in the safe use of ultrasound in medical diagnosis. Br Ins Radiol. 2000: 4-15.
17. Treeby BE, Cox BT. Modeling power law absorption and dispersion for acoustic propagation using the fractional Laplacian. J AcoustSoc Am. 2010; 127(5):2741-8. DOI: 10.1121/1.3377056.
18. Ginter S. Numerical simulation of ultrasound thermo-therapy combining nonlinear wave propagation with broadband soft tissue absorption. Ultrasonics. 2000; 37: 693-96. DOI: 10.1016/S0041-624X(00)00012-3.
19. Soneson JUS. Food and Drug Administration (FDA) Protecting and Promoting Your Health. Available from: http://www.FDA.com Updated in: 2011.
20. Grisey A, Yon S, Letort V, Lafitte P. Simulation of high-intensity focused ultrasound lesions in presence of boiling. Journal of Therapeutic Ultrasound. 2016; 4:11. DOI: 10.1186/s40349-016-0056-9.
21. HölscherTh, Raman R, Fisher D.J, Ahadi G, Zadicario E, Voie A. Effect of varying duty cycle and pulse width on high-intensity focused ultrasound (HIFU)-induced transcranial thrombolysis. Journal of Therapeutic Ultrasound. 2013; 1:18. DOI: 10.1186/2050-5736-1-18.
22. Bacon DR. IEEE Transe Ultrasound FerroelectFreqContorl. 1988; 35: 153-61.
23. Zeqiri B. Ultrasonics 1989; 27: 314-15.
24. Kaye and Laby. Tables of Physical and Chemical Constants. UK: National Physics Laboratory Available from: http:// www.kayelaby.npl.co.uk.
25. Sapareto S.A, Dewey W.C. Thermal dose determination in cancer therapy. Int. J. RadiatOncolBiol.Phys. 1984; 10(6): 787-800.
26. Parker KJ, Friets EM. On the measurements of shock waves. Ultrasound FerroelectFreqContorl. 1987; 34(4): 454-60.
27. DiederichCh.J, Hynynen K. Ultrasound technology for hyperthermia. Ultrasound Med Biol. 1999; 25(6): 871-87.
28. Sheu T.W.H, Solovchuk M.A, Chen A.W.J, Thiriet M. On an acoustics-thermal-fluid coupling model for the prediction of temperature elevation in liver tumor. Int J Heat Mass Transf. 2011; 54(17-18): 4117-26. DOI: 10.1016/j.ijheatmasstransfer.2011.03.045.
29. Carling U, Barkhato L, Courivaud F, Courivaud F, Storås T, Doughty R, et al. MRg-HIFU – experimental perivascular volumetric ablation in the liver. Journal of Therapeutic Ultrasound. 2015; 3(suppl 1): O83. DOI: 10.1007/978-3-319-22536-4_3.
30. Wackerle D, Celik H, Kinnaird D, Yang D, Eranki A, Oetgen M, et al. The optimization of treatment planning and ablation rate improvements of feasibility of pediatric MR-HIFU applications. Journal of Therapeutic Ultrasound. 2015; 3(suppl 1): p77. DOI: 10.1186/2050-5736-3-S1-P77.
31. Kinnaid D, Wackerle D, Yang D, Oetgen M, Eranki A, Kim A, et al. Treatment planning and patient positioning for MR-guided high intensity focused ultrasound treatment: a systematic approach. Journal of Therapeutic Ultrasound. 2015; 3(suppl 1): p65. DOI: 10.1186/2050-5736-3-S1-P65.